



**NATIONAL TRANSPORTATION SAFETY BOARD**  
Office of Aviation Safety  
Washington, D.C. 20594

**AIRWORTHINESS GROUP FACTUAL REPORT ADDENDUM 6**  
**MLG FINITE ELEMENT MODEL**

July 21, 2008

**A. ACCIDENT      DCA06FA058**

Location:            Memphis, Tennessee  
Date:                July 28, 2006  
Time:                1125 Central Daylight Time (CDT)  
Aircraft:            FedEx Express Flight 630, McDonnell-Douglas (Boeing) MD-10-10F,  
                              N391FE

**B. AIRWORTHINESS GROUP**

Chairman:           Clinton R. Crookshanks  
                             National Transportation Safety Board  
                             Denver, Colorado

Member:            Steve Cole  
                             FedEx  
                             Memphis, Tennessee

Member:            Vikki Anderson  
                             Federal Aviation Administration  
                             Washington, District of Columbia

Member:            Joe Bracken  
                             Air Line Pilots Association  
                             Herndon, Virginia

Member:            Dan Reynolds  
                             The Boeing Company  
                             Long Beach, California

Member: Vin Bui  
The Boeing Company  
Long Beach, California

Member: Sudhir Sheth  
The Boeing Company  
Long Beach, California

Member: Sunil Jinadasa  
The Boeing Company  
Long Beach, California

## C. **DETAILS OF THE INVESTIGATION**

### 1.0 Finite Element Model Development

In order to accurately determine the stresses in the vicinity of the air filler valve bore, the group decided to develop a finite element model of the MD-10-10F main landing gear (MLG). The task was given to the Boeing Company since they had the capabilities and staff to undertake the effort but was supervised by the group. It was decided early on that the ABAQUS non-linear, large displacement solver would be used to perform the analysis. The pre- and post- processing of the model was performed in PATRAN. The finite element model (Figure 1) included a detailed outer cylinder, a simplified piston, and a simplified side brace. The detailed solid model of the outer cylinder was developed in Unigraphics using the nominal drawing dimensions. The geometry in the vicinity of the filler valve bore was carefully modeled to include all fillets and radii. The threads in the bore were not included since their location was outside the load path in the outer cylinder. The geometry at the bottom of the outer cylinder in the vicinity of the torque link attach lug was simplified to eliminate unnecessary material and provide a simple surface to apply the input torque loads. The outer cylinder model was meshed using C3D10 Tetrahedral elements and contained 167,302 elements and 272,741 nodes in its final configuration. The mesh density was increased in the area of the air filler valve bore to provide increased accuracy of the results. See Figures 2-5 for detailed views of the mesh at the upper lugs, air filler valve bore and lower lug. The piston was included in the overall model so that the compliance of the assembly was correct, but the piston itself was simplified considerably. The simplified piston was modeled using simple S4R5 shell elements. The upper and lower bearings were modeled using solid C3D8 brick elements. The upper bearing (Figure 6) was connected directly to the piston with tie constraints on the inner surface and allowed to slide along the outer cylinder on the outer surface. The lower bearing (Figure 7) was connected to the outer cylinder with tie constraints along the outer surface and allowed to slide along the piston on the inner surface. The sliding contact at the bearings was permitted at the nominal drawing dimensions. The side brace was modeled as a simple beam connected to a shell element representation of the lower lug. The spacer and nut were modeled as solid element rings on the inboard and outboard side, respectively, of the lower lug (Figure 8). No play was allowed between the spacer, lug, and nut at the side brace attach point. The lower end of the piston was simplified but did include the truck beam attach clevis. The truck beam pivot pin was modeled as a rigid cylindrical surface through the clevis. The landing gear input loads were applied at a point, P, that was located

midway between the clevis at the center of the rigid cylinder (Figure 9). The point P was rigidly attached to the cylinder. The starting position of the MLG model was the strut extension under nominal static load assuming a correctly serviced strut.

The boundary conditions were selected to represent the normal installation of the MLG on the airplane. The upper lugs at the forward and aft trunnions were restrained radially on the inner surfaces and axially at the forward and aft faces. The drag loads were reacted at the faces of the trunnion lugs based on the loading direction input and the drawing tolerances. The drawing clearances at the trunnion lugs could result in load transfer to either one or both lugs. Examination of the stresses around the air filler valve bore indicated that they were not sensitive to the support location. The top of the side brace was restrained from movement in all three directions with a pin connection. The point P was restrained to prevent rotation and to define the vertical position or strut extension.

For the various airplane loading conditions required, Boeing used their proprietary Landing Gear Internal Load Distribution computer program to calculate the following forces and moments at point P and the strut extension.

- V – Vertical Load
- D – Drag Load
- S – Side Load
- MVP – Vertical Moment
- MDP – Drag Moment
- MSP – Side Moment
- SE<sub>out</sub> – Strut Extension

These forces and moments were then transformed to the FEM input loads using the following equations.

A 1000 psi internal strut pressure was applied to the FEM to determine the reaction on the upper flange of the outer cylinder. This yielded a specific pressure on the flange for the static case of 6858.7 psi. Utilizing this internal flange pressure and the area of the flange, the vertical load that must be reacted at the piston flange was calculated to be 118,286.101 lb. Since the vertical equivalent load is linear, the ratio between the internal pressure and vertical load will remain constant. The vertical load, V, from the landing gear program was transformed to a vertical equivalent pressure, P<sub>V</sub>, over the upper flange area using the ratio:

$$P_V = V \frac{6858.7 \text{ psi}}{118286.101 \text{ lb}}$$

It was decided to input the vertical moment, MVP, from the landing gear program at the torque link-bushing interface. In order to get about a 10,000 in-lb vertical moment, a pressure of about 76.233 psi was required at the bushing interface. Utilizing this pressure the resultant moment about the vertical axis of the gear at point P was calculated by the FEM to be 9,999.96484 in-lb. Since the moment is linear, the ratio will remain constant. The vertical moment, MVP, was transformed to a vertical moment equivalent pressure, P<sub>MV</sub>, over the bushing interface area on the torque link attach lug at the bottom of the outer cylinder using:

$$P_{MV} = MVP \frac{76.233 \text{ psi}}{9999.96484 \text{ in} - \text{lb}}$$

Utilizing the same case with the bushing interface pressure of 76.233 psi, the side load produced at the bushing interface was calculated to be 1075.3927 lb. Since the side load is linear, the ratio will remain constant. The total equivalent side load,  $S_{eq}$ , was calculated as the side load (S) from the landing gear program minus the side load due to applying the vertical moment as a pressure at the torque link flange.

$$S_{eq} = S - P_{MV} \frac{1075.3927 \text{ lb}}{76.233 \text{ psi}}$$

Again, utilizing the same case with the bushing interface pressure of 76.233 psi, the drag moment was calculated to be 27161.3574 in-lb. The ratio of the pressure and moment will remain constant due to linearity. The equivalent drag moment,  $MD_{eq}$ , was calculated as the drag moment, MDP, from the landing gear program minus the moment induced by applying the vertical moment at the torque link attach.

$$MD_{eq} = MDP - P_{MV} \frac{27161.3574 \text{ in} - \text{lb}}{76.233 \text{ psi}}$$

The drag load, D, and side moment, MSP, were input directly to the FEM at point P

The model was built to the dimensions in the assembly drawing with a static strut extension of 4.5 in. Therefore, the strut extension, SE, input into the FEM was the static strut extension minus the strut extension output from the landing gear program.

$$SE = 4.5 - SE_{out}$$

The strut internal pressure,  $P_s$ , calculated by the program was input directly to the FEM as a pressure applied directly to the inner surface of the outer cylinder.

A mesh refinement study of the full model indicated that the mesh in the air filler valve area was too coarse to accurately capture the local strains for stresses in the plastic range. The mesh refinement was initially applied to the full model but the run times became excessive so a submodel was developed to save on computation time. The submodel included the air filler valve bore and the outer wall of the cylinder with a diameter of 5.6 inches about the center of the bore. The submodel mesh was refined from the full model and further refinement of the mesh occurred from a diameter of 1.1 inches to the bore surface. The final mesh size at the bore surface was 0.024" x 0.024" compared to the nominal mesh size in the full model of 0.25" x 0.25". The transition at the inner edge of the bore was modeled as a 0.015" x 0.015" chamfer in the submodel. The submodel utilized C3D10 tetrahedral elements and was comprised of 122,476

elements and 175,322 in its final configuration. Like the full model, the ABAQUS non-linear, large displacement solver was used for the submodel. The full model was run and output the displacements at the nodes along the submodel boundary (5.6 inches diameter). These displacements were then used as the input boundary conditions for the submodel. Using displacement boundary conditions will be accurate as long as the stresses at the boundary remain below the material yield stress, which they do for these cases. The internal strut pressure was applied at the inner surface of the outer cylinder and at the bore surface up to the point where the threads would begin.

The following material properties for 300M steel were input to the FEM from Douglas Material Specification (DMS) 1935.

$$\begin{aligned}F_{ty} &= 220 \text{ ksi} \\F_{tu} &= 280 \text{ ksi} \\E &= 29,000 \text{ ksi}\end{aligned}$$

The stress-strain relationship for 300M was taken from Boeing Laboratory Test Data, Test No. 24596. Since ABAQUS requires true stress versus true strain, the engineering stress-strain curve was converted using the following formulas:

$$\begin{aligned}\sigma_{true} &= \sigma \times (1 + \varepsilon) \\ \varepsilon_{true} &= \ln(1 + \varepsilon)\end{aligned}$$

## 2.0 Calibration of the Finite Element Model

After the test instrumentation was installed on aircraft N357FE, calibration runs were performed to check out the instrumentation<sup>1</sup>. Static engine run-ups were performed at both 80% and 90% N1 for several seconds while gathering data. Using the generic engine thrust curves for the CF6-6D engines the thrust was obtained and input into the Boeing Landing Gear Internal Load Distribution computer program to obtain the loads and moments on the landing gear. The gear loads and moments were transformed as described above and input to the FEM. See Table 1 for the loads output from the Boeing MLG program and the input loads to the FEM. The model was run to convergence at both the 80% and 90% thrust levels. The calculated strain at each node within the gage footprint area at the two linear gage locations below the air filler valve on the aft side of the strut (XL2 and XL6<sup>2</sup>) and the corresponding two linear gages on the forward side of the strut (XL1 and XL5) for both the left and right MLG was output from the model. The mean of these calculated strain values was obtained from the minimum and maximum values at each gage location and compared to the average measured strain gage data recorded during the test. See Table 2 for the comparison of the measured and calculated strain values. The calculated strains from the FEM ranged about 8% to 20% lower than the strains measured with the instrumentation. The average under prediction was about 14%. The group decided that all calculated stresses output from the FEM would be increased by 10% to get closer to the actual loads on the MLG.

---

<sup>1</sup> See Airworthiness Group Factual Report Addendum 4 – In Service Evaluation for detailed information.

<sup>2</sup> X will be either L or R depending on which landing gear the strain gage is installed on, left or right.

### 3.0 Input Load Cases

The original certification fatigue landing and braking spectrums were utilized in the FEM. The certification spectrums were based on 150,000 total flights. The fatigue landing loads were broken up into 62 conditions, 10 each for the pre-flight taxiing at take-off weight with  $\mu=0.25^3$ , pre-flight taxiing at take-off weight with  $\mu=0.75$ , landing rollout and post flight taxiing at landing weight with  $\mu=0.25$ , landing rollout at landing weight with  $\mu=0.5$ , hard braking at landing weight with  $\mu=0.75$ , and engine run-up at takeoff weight, and 2 conditions for maintenance engine run-up. Each condition had one of 10 center-of-gravity geometries, a range of vertical and drag loads and a number of expected cycles in service (out of 150,000). The fatigue loads and cycles for the conditions were then lumped into 5 different braking spectrums.

- Brake A: Comprised of 9 conditions, Vertical load on the MLG ( $V_M$ ) from 144,000 lb to 136,000 lb, Drag Load (D) from 0 to 34,000 lb, and 331,036 total cycles.
- Brake B: Comprised of 11 conditions,  $V_M$  from 175,000 lb to 162,000 lb, D from 0 to 40,000 lb, and 516,594 total cycles.
- Brake C: Comprised of 18 conditions,  $V_M$  from 165,000 lb to 159,000 lb, D from 0 to 62,000 lb, and 220,510 total cycles.
- Brake D: Comprised of 10 conditions,  $V_M$  from 156,000 lb to 140,000 lb, D from 0 to 72,000 lb, and 49,555 total cycles.
- Brake E: Comprised of 14 conditions,  $V_M$  from 170,000 lb to 145,000 lb, D from 0 to 110,000 lb, and 239 total cycles.

The landing fatigue cases were selected based on load levels from the certification work on the airplane. The group chose the cases that produced the highest loads on the MLG. Fourteen total cases were used for the calibration of the FEM. The naming convention for the cases is the two letter type of case, either SU or SB. SU is for the spin up condition when the wheels first contact the ground and the landing gear is pulled aft causing a compressive stress on the aft side of the cylinder. SB is the spring back condition where the gear moves forward after being deflected aft by the spin up. This produces a tension stress on the aft side of the cylinder. The next number, 0, 6, or 12, is the pitch angle at the time of touchdown. For this analysis, only the level landing case ( $\alpha = 0$ ) was used since it produces the highest loads on the MLG. The level landing was assumed to occur 37,500 times in 150,000 landings per the original certification. The next number is the sink rate in feet per second. The following lists the conditions used in the analysis.

SU0 2.5 1A	SB0 2.5 1A
SU0 3.5 1A	SB0 3.5 1A
SU0 4.5 1A	SB0 4.5 1A
SU0 5.5 1A	SB0 5.5 1A
SU0 6.5 1A	SB0 6.5 1A
SU0 7.5 1A	SB0 7.5 1A
SU0 8.5 1A	SB0 8.5 1A

The lumped braking spectrums and the landing spectrums were each input to the Boeing MLG

---

<sup>3</sup>  $\mu$  is the coefficient of static friction between the tires and runway and is a measure of the braking effectiveness.

program to obtain the equivalent loads at point P (Table 3) which were then transformed to the input loads, at point P, required for the FEM (Table 4). The full FEM was run to convergence followed by the submodel and the strain at the L6 location 3.60” below the air filler valve bore, submodel principal stress in the hole, and equivalent plastic strain (if there was yielding) were output. The L6 stress was calculated using Young’s modulus. For the cases where there was significant yielding, the FEM was unloaded and the principal hole stress was output. The results are shown in Table 5. For the cases where there was no or minimal yielding (all cases except the three Brake E cases) the material acts linear and the stress ratio between the L6 stress and the principal hole stress can be calculated. This stress ratio was consistently about 2.6 so this value will be used to factor the L6 strain to hole stress for the ISE loads. The Brake E case produced yielding at the hole with an input drag load of 113 kips<sup>4</sup>. The highest loads evident during the ISE were 95 kips, 106 kips, and 153 kips. Two additional cases appear in the tables, Brake E to 100K and Brake E to 153K, that represent these high loads seen during the ISE and will be discussed in detail in the Airworthiness Group Factual Report Addendum 7 – Main Landing Gear Loads.

---

<sup>4</sup> Kilopounds (1000 pounds)

	V (lb)	D (lb)	S (lb)	MVP (in-lb)	MDP (in-lb)	MSP (in-lb)	Strut Extension (in)	Strut Air Pressure (psi)
Cali_80%N 1	135600	22210	0	-1149	6646	441349	3.67	1306
Cali_90%N 1	134100	30604	0	-1569	6508	603452	3.727	1291
	Pv (psi)	D (lb)	Seq (lb)	Pmv (psi)	MDeq (in-lb)	MSP (in-lb)	SE (in)	Ps (psi)
Cali_80%N 1	7862.6 3	22210.0 0	-123.56	8.76	3525.1 5	441349.0 0	0.830	1306
Cali_90%N 1	7775.6 5	30604.0 0	-168.73	11.96	2246.3 7	603452.0 0	0.773	1291

Table 1 – Output Loads from Boeing MLG Program and Input Loads to FEM for Calibration

	RL1 (µin/in)	RL2 (µin/in)	RL5 (µin/in)	RL6 (µin/in)	LL1 (µin/in)	LL2 (µin/in)	LL5 (µin/in)	LL6 (µin/in)
Cali_80%N 1								
Measured	750	-1231	703	-1077	731	-1169	670	-1060
Calculated	608	-1037	560	-918	608	-1037	560	-918
%error	-19	-16	-20	-15	-17	-11	-16	-13
Cali_90%N 1								
Measured	1022	-1581	959	-1378	995	-1507	914	-1355
Calculated	879	-1384	808	-1219	879	-1384	808	-1219
%error	-14	-12	-16	-12	-12	-8	-12	-10

Table 2 – Comparison of Measured and Calculated Strain for Calibration



Condition	V	D	S	MVP	MDP	MSP	Strut extension	Strut Air Pressure
Brake A	140823	35156	0	-1548	5680	830167	3.47	1354
Brake B	167507	41360	0	-1744	6391	955798	2.67	1613
Brake C	164405	64108	0	-2739	6326	1485215	2.75	1583
Brake D	144759	74448	0	-3245	5708	1752214	3.33	1394
Brake E	149929	113740	0	-4899	5767	2665960	3.16	1444
Brake E to 100K	149929	100000	0	-4899	5767	2665960	3.16	1444
Brake E to 153K	149929	153000	0	-4899	5767	2665960	3.16	1444
SU0 2.5 1A	33734	33630	2346	-41755	-8156	16876	19.40	294
SB0 2.5 1A	30908	-13418	-936	-6045	5965	-6712	18.60	298
SU0 3.5 1A	40837	45106	3147	-61981	-11168	22674	17.30	333
SB0 3.5 1A	41676	-25083	-1750	-16519	9889	-12557	15.80	369
SU0 4.5 1A	53073	62184	4338	-105102	-3424	31353	15.60	373
SB0 4.5 1A	56049	-44120	-3078	-46029	7563	-22134	13.80	424
SU0 5.5 1A	68940	60607	4228	-77807	-3058	30493	14.60	401
SB0 5.5 1A	72790	-45579	-3179	-37684	8575	-22851	12.30	477
SU0 6.5 1A	68892	57777	4030	-70939	-2692	29054	18.70	286
SB0 6.5 1A	92437	-35066	-2446	-17083	8312	-17554	11.30	524
SU0 7.5 1A	80471	68927	4808	-86324	-3964	34704	18.00	318
SB0 7.5 1A	115924	-32007	-2233	-12496	3845	-16015	11.00	539
SU0 8.5 1A	96133	83049	5793	-107096	-3168	41878	17.20	335
SB0 8.5 1A	141069	-51516	-3594	-27709	4380	-25806	11.00	537

Table 3 – Fatigue Load Case Output from Boeing MLG Model

Condition	Pv (psi)	D (lb)	Seq (lb)	Pmv (psi)	MDeq (in-lb)	MSP (in-lb)	SE (in)	Strut Air Pressure (psi)
Brake A	8165.5	35156	-166.5	11.8	1475	830167	1.03	1354
Brake B	9712.7	41360	-187.5	13.3	1654	955798	1.83	1613
Brake C	9532.9	64108	-294.6	20.9	-1114	1485215	1.75	1583
Brake D	8393.7	74448	-349.0	24.7	-3106	1752214	1.17	1394
Brake E	8693.5	113740	-526.8	37.3	-7539	2665960	1.34	1444
Brake E to 100K	8693.5	100000	-526.8	37.3	-7539	2665960	1.34	1444
Brake E to 153K	8693.5	153000	-526.8	37.3	-7539	2665960	1.34	1444
SU0 2.5 1A	1956.0	33630	-2144.3	318.3	-121569	16876	0.60	294
SB0 2.5 1A	1792.2	-13418	-1586.1	46.1	-10454	-6712	1.40	298
SU0 3.5 1A	2367.9	45106	-3518.4	472.5	-179517	22674	2.70	333
SB0 3.5 1A	2416.5	-25083	-3526.4	125.9	-34979	-12557	4.20	369
SU0 4.5 1A	3077.4	62184	-6964.6	801.2	-288896	31353	4.40	373
SB0 4.5 1A	3249.9	-44120	-8027.9	350.9	-117458	-22134	6.20	424
SU0 5.5 1A	3997.4	60607	-4139.3	593.1	-214393	30493	5.40	401
SB0 5.5 1A	4220.7	-45579	-7231.5	287.3	-93780	-22851	7.70	477
SU0 6.5 1A	3994.6	57777	-3598.8	540.8	-195373	29054	1.30	286
SB0 6.5 1A	5359.9	-35066	-4283.1	130.2	-38088	-17554	8.70	524
SU0 7.5 1A	4666.0	68927	-4475.3	658.1	-238433	34704	2.00	318
SB0 7.5 1A	6721.7	-32007	-3576.8	95.3	-30096	-16015	9.00	539
SU0 8.5 1A	5574.2	83049	-5724.1	816.4	-294056	41878	2.80	335
SB0 8.5 1A	8179.7	-51516	-6573.8	211.2	-70882	-25806	9.00	537

Table 4 – Fatigue Load Case Input to FEM

Model Results					Unloaded Case		
Condition	L6 strain ( $\mu\text{in/in}$ )	L6 Stress (psi)	Principal Hole Stress (psi)	Equivalent Plastic Strain	Stress Ratio Hole/L6	Submodel Principal Hole Stress (psi)	Equivalent Plastic Strain
Brake A	-1435	-41615	-107698	0	2.59		
Brake B	-1663	-48227	-125032	0	2.59		
Brake C	-2506	-72674	-189226	0	2.60		
Brake D	-2915	-84535	-215564	0.0002	2.55		
Brake E	-4390	-127310	-271121	0.0035	2.13	68218	0.0035
Brake E to 100K	-4000	-116000	-260304	0.0023	2.24	47664	0.0023
Brake E to 153K	-5530	-160370	-295217	0.0075	1.84	135959	0.0075
SU0 2.5 1A			-91885	0			
SB0 2.5 1A	441	12789	33295	0	2.60		
SU0 3.5 1A			-120127	0			
SB0 3.5 1A	821	23809	61564	0	2.59		
SU0 4.5 1A			-162084	0			
SB0 4.5 1A	1432	41528	107052	0	2.58		
SU0 5.5 1A			-156536	0			
SB0 5.5 1A	1453	42137	108350	0	2.57		
SU0 6.5 1A			-156099	0			
SB0 6.5 1A	1090	31610	81248	0	2.57		
SU0 7.5 1A			-184834	0			
SB0 7.5 1A	985	28565	73223	0	2.56		
SU0 8.5 1A			-215059	0.0002			
SB0 8.5 1A	1616	46864	119796	0	2.56		

Table 5 – FEM Results for Fatigue Load Cases

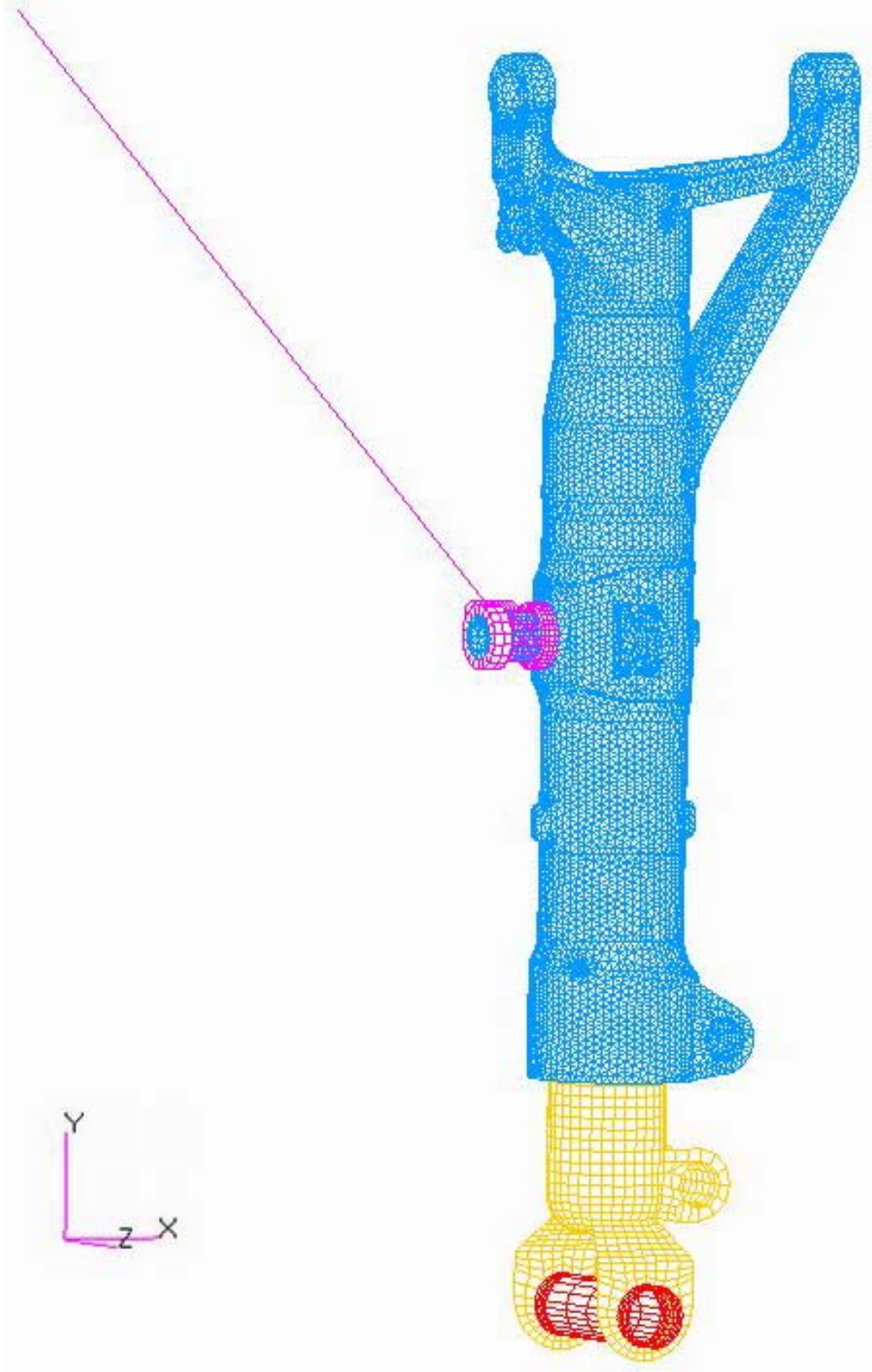


Figure 1 – Finite Element Model of the MD-10 Main Landing Gear

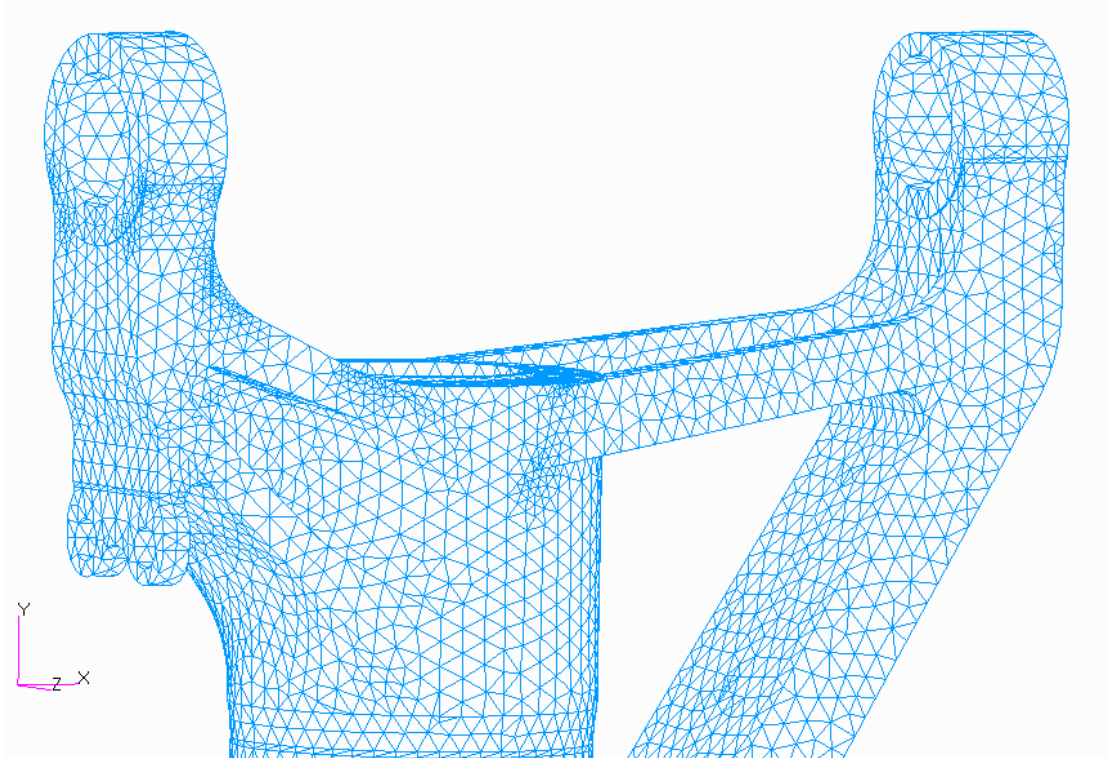


Figure 2 – Detailed Mesh at Upper Lugs

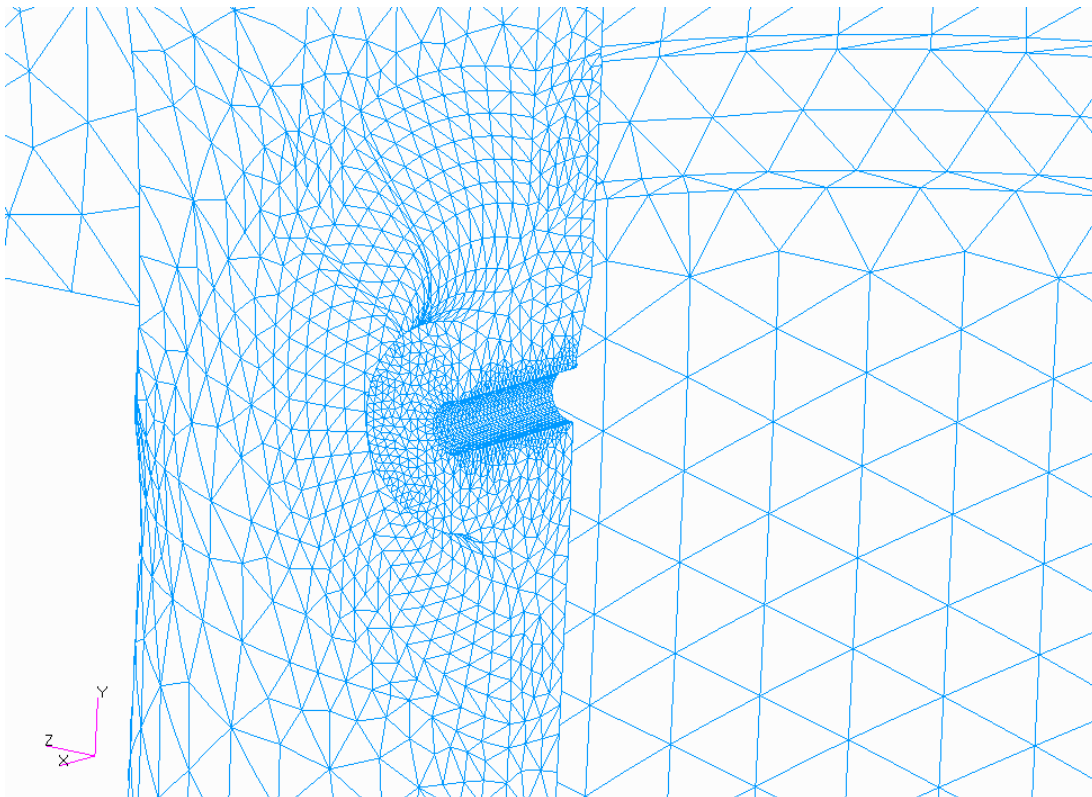


Figure 3 – Increased Mesh Density at Filler Valve Bore from Outside

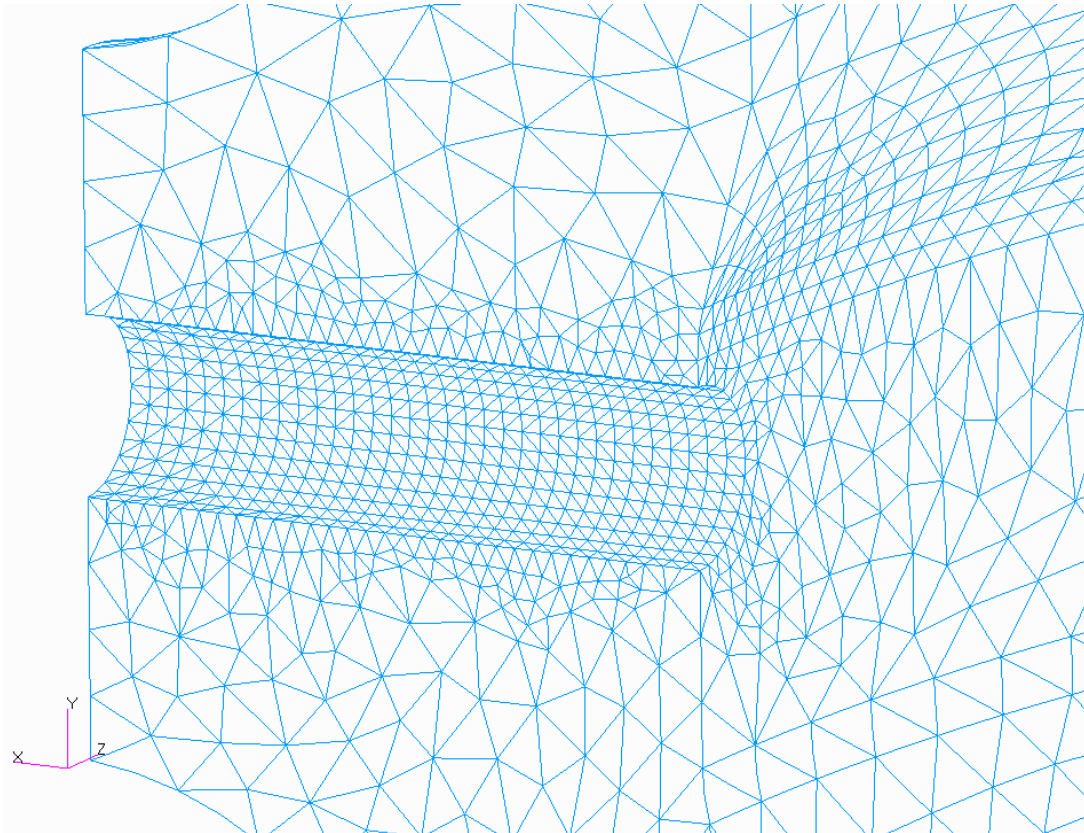


Figure 4 – Valve Bore from Inside

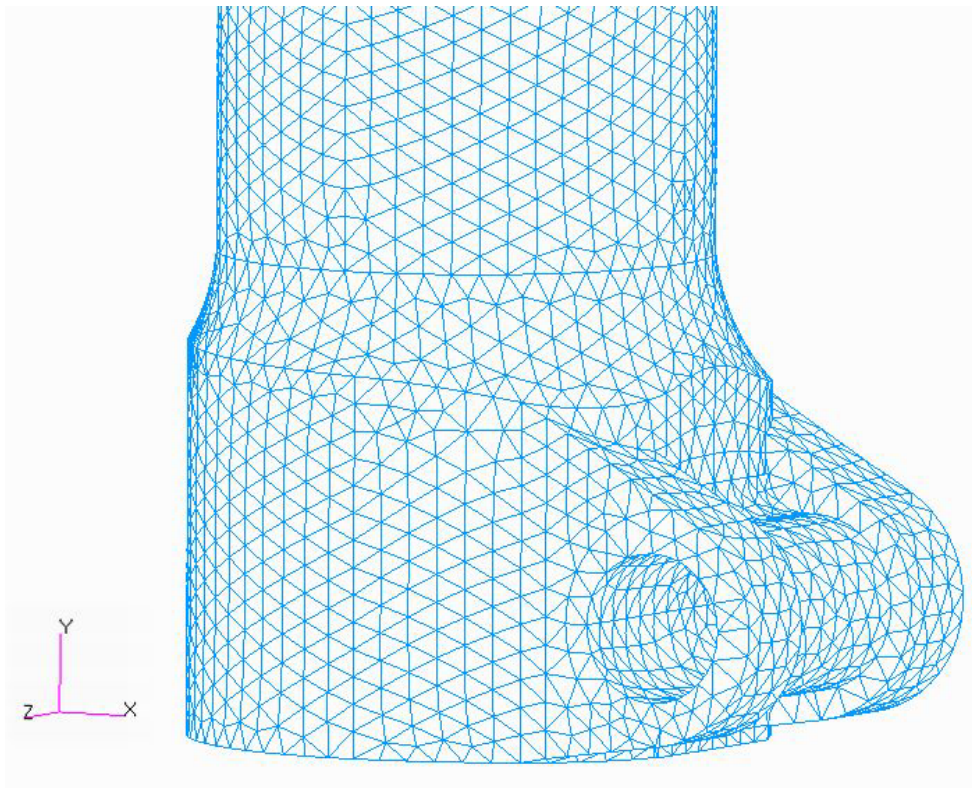


Figure 5 – Simplified Torque Lug at Lower Outer Cylinder

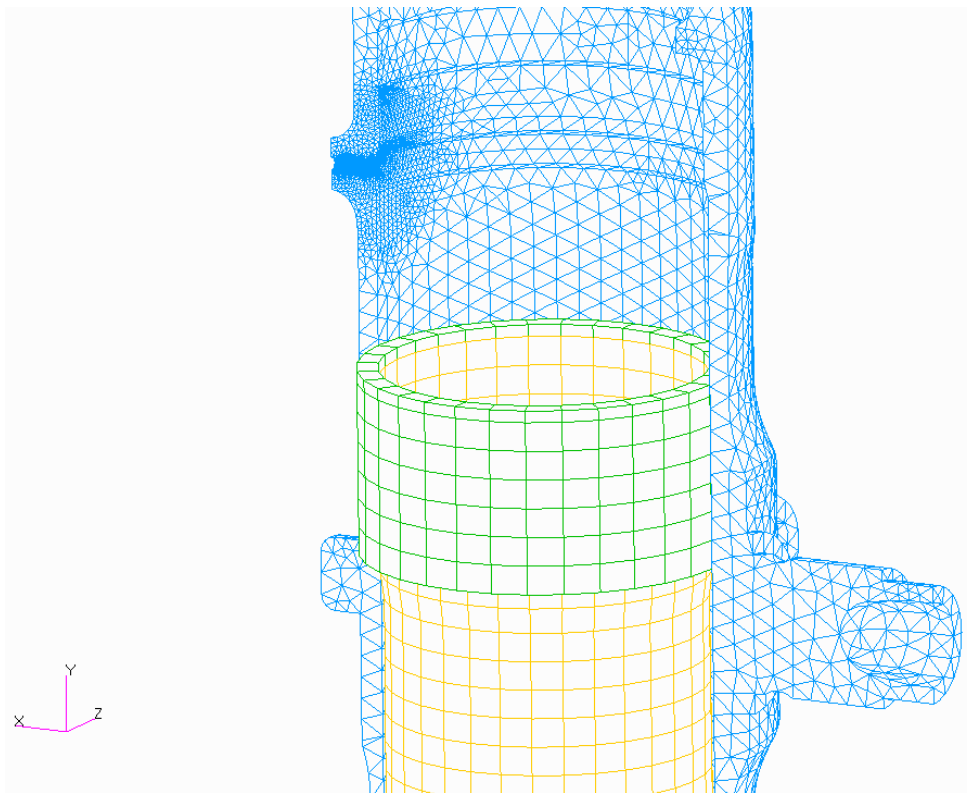


Figure 6 – Upper Bearing

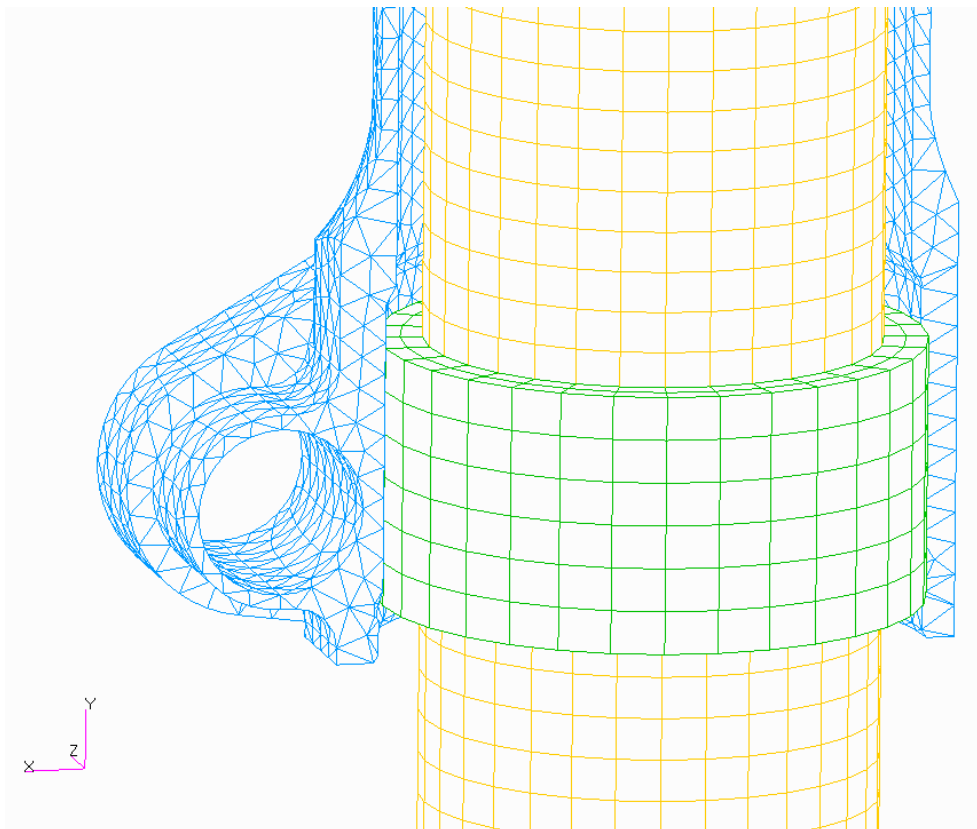


Figure 7 – Lower Bearing

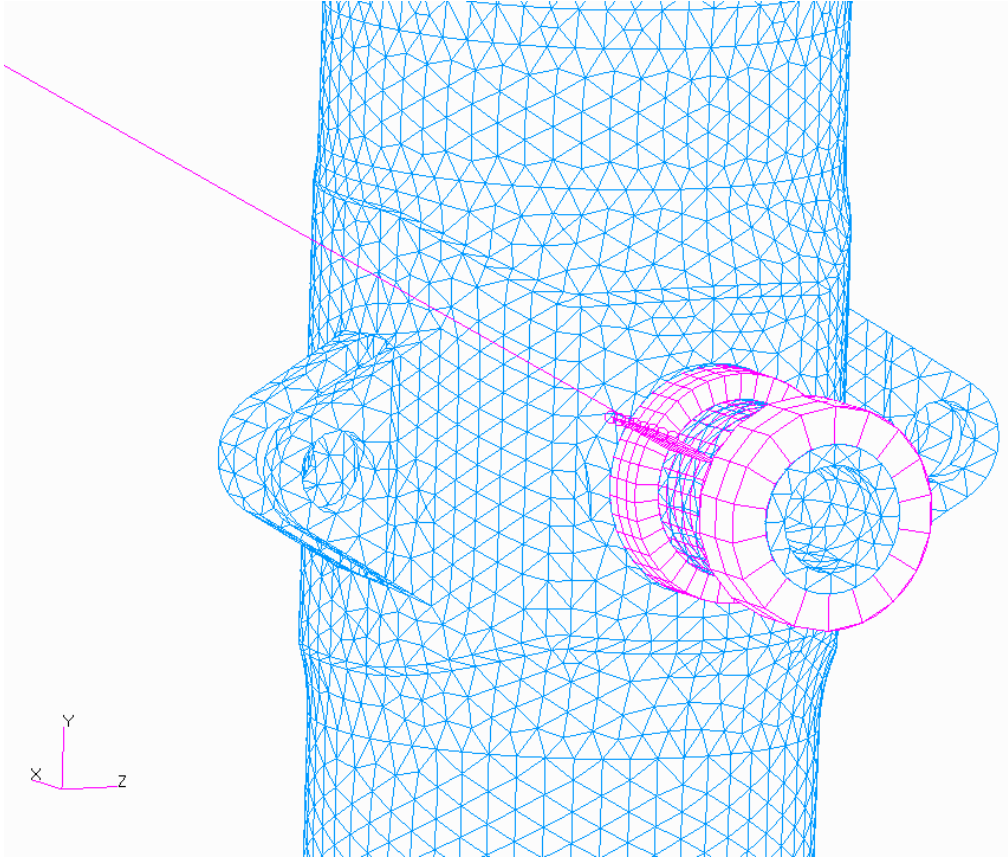


Figure 8 – Side Brace Lower Lug, Spacer and Nut

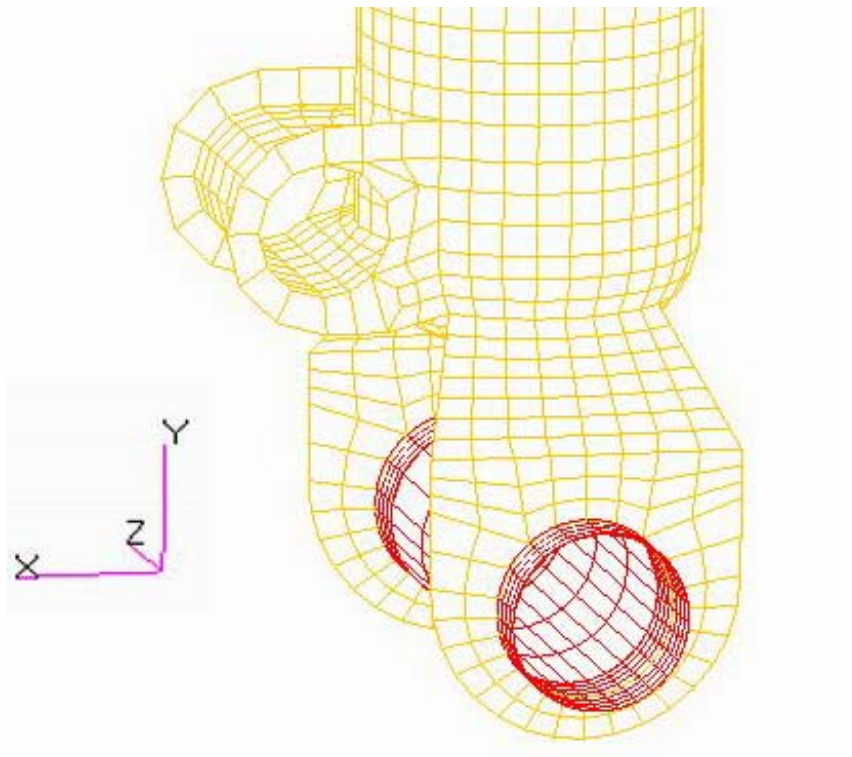


Figure 9 – Truck Beam Pivot Joint